International Immunopharmacology 76 (2019) 105921

Contents lists available at ScienceDirect

International Immunopharmacology

journal homepage: www.elsevier.com/locate/intimp

BET bromodomain inhibitor JQ1 promotes immunogenic cell death in tongue squamous cell carcinoma

Miao Wang[a,b], Lu Zhao[a,c], Dongdong Tong[a,b], Linrui Yang[a,b], Hongjie Zhu[a,b], Qing Li[a,b,*], Fenghe Zhang[a,b,*]

[a] Shandong Provincial Key Laboratory of Oral Tissue Regeneration, School of Stomatology, Shandong University, Jinan, Shandong Province, China
[b] Department of Oral and Maxillofacial Surgery, School of Stomatology, Shandong University, Jinan, Shandong Province, China
[c] .Department of Stomatology, Binzhou People's Hospital, Binzhou, Shandong Province, China

ARTICLE INFO

Keywords:
Immunogenic cell death
BET inhibitor
JQ1
p-eIF2a
Tongue squamous cell carcinoma

ABSTRACT

Drug resistance substantially limits the curative capability of chemotherapy in head and neck cancers such as oral squamous cell carcinoma. Immunosuppression is considered a potential cause of drug resistance. A key discovery in the past decade is that chemotherapeutics can alter tumor cell immunogenicity via inducing release of damage-associated molecular patterns (DAMPs), including ecto-calreticulin (ecto-CALR), high mobility group box 1 (HMGB1) and ATP, causing tumor cells to die in a manner known as bona fide immunogenic apoptosis or immunogenic cell death (ICD). Intriguingly, JQ1 was found in this study to exhibit therapeutic potential in tongue squamous cell carcinoma (TSCC) by inducing ICD. JQ1 induced significant release of calreticulin (CALR), HMGB1 and ATP from Cal27 and SCC7 cells *in vitro*. Immature dendritic cells (Im-DCs) cocultured with JQ1-pretreated Cal27 cells exhibited significant upregulation of mature markers on their surface and an increase in the secretion of cytokines. *In vivo* experiments demonstrated that JQ1-pretreated dying SCC7 cells protected immunocompetent mice from rechallenge of SCC7 cells. Intravenous injection of JQ1 efficiently reduced tumor growth and increased tumor-infiltration of $CD3^+/CD8^+$ T cells in C3H mice.

1. Introduction

Immunosuppression is a major reason for tumor metastasis, drug resistance and unfavorable prognosis. However, a number of anti-tumor drugs such as anthracyclines and oxaliplatin [1,2], and photodynamic therapy (PDT) [3] have been reported to induce immunogenic death of cancer cells (ICD) that could enhance surveillance of the immune system. These drugs or therapies are capable of activating RNA-like endoplasmic reticulum kinase (PERK) and subsequently phosphorylation of eukaryotic translation initiation factor 2a (P-eIF2a), a biomarker of ICD [4,5] that is considered to correlate with calreticulin (CALR) translocation [6,7]. CALR is among the most important danger-associated molecular patterns (DAMPs) in ICD. Others include ATP and high mobility group box 1 protein (HMGB1). These DAMPs regulate immunosurveillance by providing "eat me" signals to immunocytes, particularly DCs. When binding to pattern-recognition receptors (PRRs) on immunocytes, the DAMPs trigger enhanced phagocytosis activity accompanied by a robust antitumor T-cell response and establishment of immunological memory [8–10]. Therefore, these DAMPs are regarded as the hallmarks of ICD [10,11]. In particular, multifunctional Ca^{2+} binding protein CALR is a crucial and characteristic chaperone of ICD. Knockdown of CALR or blockade of its transfer to the cell membrane severely compromises bona fide ICD [7,12]. In the majority of cases, the transfer of CALR occurs together with another ER chaperone, ERp57 [13]. A number of studies have explored the mechanisms of CALR/ERp57 complex translocation. However, due to the participation of ER stress and apoptosis during CALR transportation, the signal pathway of ecto-CALR conduction remains unclear. In addition, the mechanisms vary depending on the induction agent.

JQ1 is a membrane-permeable small molecular inhibitor of bromodomain and extra-terminal (BET) family proteins such as bromodomain containing protein 4 (BRD4) that recognizes acetylated lysine

Abbreviations: TSCC, tongue squamous cell carcinoma; ICD, immunogenic cell death; DAMPs, danger associated molecular patterns; CALR, calreticulin; HMGB1, high mobility group box 1; BET, bromodomain and extraterminal protein family; BRD4, bromodomain containing protein 4; PDT, photodynamic therapy; ER, endoplasmic reticulum; Im-DCs, immature DCs

* Corresponding authors at: Shandong Provincial Key Laboratory of Oral Tissue Regeneration, School of Stomatology, Shandong University, No. 44-1 Wenhua Road West, Jinan, China (F. Zhang).
E-mail address: zfengh@sdu.edu.cn (F. Zhang).

https://doi.org/10.1016/j.intimp.2019.105921
Received 29 June 2019; Received in revised form 15 September 2019; Accepted 15 September 2019
Available online 07 October 2019
1567-5769/ © 2019 Elsevier B.V. All rights reserved.

residues on histones and regulates the expression of c-Myc [14,15]. Specifically, JQ1 selectively displaces the BET proteins BRD2, BRD3, BRD4 and BRDT from chromatin by inhibiting the bromodomain of BET proteins that interacts with histones, suppressing gene expression and interfering with mRNA elongation [16,17]. In this way, JQ1 represses tumor proliferation in a variety of neoplasia models including pancreatic carcinoma [18], non-small cell lung cancer [19], neuroblastoma [20], nut mid-line carcinoma [21], etc.

Tongue squamous cell carcinoma (TSCC) is the most common malignant tumor of the oral cavity which has poor prognosis due to the extraordinary levels of local invasiveness and early lymphatic metastasis. The five-year survival rate for TSCC from 2002 to 2006 has been estimated to be approximately 65% [22,23], remaining the same in the current decade. It is influenced by smoking, radiation and many different clinical characteristics [24]. We have found that JQ1 is able to suppress the expression levels of the bromodomain protein BRD4 in TSCC resulting in inhibition of tumor proliferation and metastasis similar to the findings of previous studies [25–27]. Interestingly, we found that JQ1 was only capable of inducing mild apoptosis in TSCC cells *in vitro* but efficiently reduced tumor growth in immunocompetent SCC mouse models, implying that administration of JQ1 leads to some form of immune system activation. Hence, this study was designed to explore if BRD4 inhibitor JQ1 triggered release of DAMPs in TSCC and whether it was able to provoke an enhanced anti-tumor immune response both *in vitro* and *in vivo*.

2. Materials and methods

2.1. Reagents

JQ1 (Targetmol, Boston, MA, USA) was dissolved in dimethyl sulfoxide (DMSO) (Sigma, St. Louis, MO, USA). Control group cells were incubated with corresponding concentrations of DMSO.

2.2. Cells and animals

The oral squamous cancer cell line Cal27 (Procell Life Science & Technology, Wuhan, China) was cultured in DMEM (Hyclone) supplemented with 10% fetal bovine serum (FBS, Gibco. Grand Island, NY, USA) at 37 °C in a humidified incubator containing 5% CO_2. SCC7 murine tongue squamous cell carcinoma cells, gifted by Dr. Li, Shandong University Stomatology Academy, were maintained in RPMI 1640 (Hyclone) supplemented with 10% FBS. Five-week-old female C3H/HeNcrl (C3H) mice and Nu/Nu nude mice were purchased from Beijing Vital River Laboratory Animal Technology Co. (Beijing, China). All animals were maintained under specific pathogen-free conditions. All animal experiments were approved by the Research Ethics Committee of Shandong University Dental School (GD201821).

2.3. Cell proliferation assay

The proliferation rate of Cal27 and SCC7 cells was quantified using a Cell Counting Kit-8 (EnoGene, Nanjing, China) in accordance with the manufacturer's instructions. Cells (100 μL) were plated in 96-wells plates at a density of 5000 cells/well and incubated for 24 h, then treated with various concentrations of JQ1. After 12 h, 24 h, 36 h and 48 h, the culture medium was replaced with FBS-free DMEM and 10 μL CCK-8 solution were added to each well. The plate was then incubated at 37 °C for 1-3 h in the dark and the OD levels at 450 nm measured using a microplate reader (BMG SPECTROstar^{nano}, BMG Labtech GmbH, Ortenberg, Germany).

2.4. Cell cycle analysis

Cal27 or SCC7 cells were seeded in 6-well plates at a density of 10^5 cells/well. After culture for 24 h, the cells were treated with 4 μM (Cal27) or 2 μM (SCC7) JQ1 for 24 h then harvested and fixed with 70% ethyl alcohol. On the following day, the cells were stained with propidium iodide (50 μg/mL) containing 0.25 mg/mL RNAse (BD Pharmingen, Franklin Lakes, NJ, USA). Cell cycle distribution was analyzed using a BD Accuri^{TM} C6 Plus flow cytometer (BD Biosciences, San Jose, CA, USA).

2.5. Apoptosis

Cal27 or SCC7 cells were seeded in 6-well plates at a density of 1×10^5 cells per well. After incubation for 24 h, JQ1 was added to each well and incubated for 8 h, 24 h and 48 h. Cell apoptosis was assessed by double staining with PE-conjugated Annexin V and 7-AAD (Apoptosis detection kit I, BD Pharmingen, Franklin Lakes, NJ, USA) in accordance with the manufacturer's instructions. Apoptosis of each cell was determined using a BD Accuri™ C6 Plus flow cytometer. Cell populations in the upper and lower right quadrants (Annexin V^+/7-AAD^-, Annexin V^+/7-AAD^+) were quantified.

2.6. RNA isolation and quantitative RT-PCR (qRT-PCR)

Total RNA was extracted using TRIzol™ reagent (Invitrogen, Shanghai, China) using conventional chloroform/isopropanol-based methods [28] and reverse transcribed to create cDNA in two steps using PrimeScript™ RT Master Mix (Takara Bio, Shiga, Japan). qRT-PCR was conducted using a 20 μL reaction system with a SYBR® Premix Ex Taq™ kit (Takara Bio, Shiga, Japan) in a LightCycler Roche 480 instrument (Roche, Basel, Switzerland). β-Actin served as the endogenous reference gene. Relative mRNA expression was calculated using the $-\Delta\Delta C_T$ method. Primers sequences were as follows:

BRD4: Forward: 5′-CGTCAAGCTGAACCTCCCTG-3′,
Reverse: 5′-TGTCATCTCCAGGCTTGTTGT-3′.
β-Actin: Forward: 5′-CATGTACGTTGCTATCCAGGC-3′,
Reverse: 5′-CTCCTTAATGTCACGCACGAT-3′.

2.7. Flow cytometric analysis of ecto-CALR/ERp57

Cal27 or SCC7 cells were seeded into 6-wells plates at a density of 10^5 cells/well. After incubating at 37 °C in an atmosphere containing 5% CO_2 for 24 h, JQ1 was added to the cells then incubated for 4 h. The samples were then fixed with 1% paraformaldehyde (PFA, Bosterbio, Wuhan, China) for 5 min prior to staining with a fluorescent antibody. The samples were then washed with cold PBS and the supernatants carefully aspirated. Either anti-calreticulin or anti-ERp57 antibody (Abcam, Cambridge, MA, USA), diluted 1:50 with 1% BSA/PBS, were added to each sample and incubated at room temperature for 40 min in the dark. After washing three times, 100 μL secondary antibody conjugated with Alexa Fluor® 488 (Abcam, Cambridge, MA, USA), diluted 1:2000, were added to each sample and incubated at 4 °C for 20 min. Finally, the cells were washed 3 times and resuspended in 200 μL PBS. Five μL 7-AAD were added to each sample (0.25 μg/test) 5 min prior to detection by flow cytometry to exclude dying cells.

2.8. DCFH assay

A DCFH assay was performed to detect ROS levels. Cal27 or SCC7 cells were incubated in a 6-well plate with JQ1 for 1–3 h. The supernatant was then discarded and the cells were incubated in serum-free medium containing 10 μM dichloro-dihydro-fluorescein diacetate (DCFH-DA) probe (Sigma, St. Louis, MO, USA) at 37 °C. After 30 min, the cells were collected, washed, resuspended in 400 μL PBS and immediately analyzed by flow cytometry at 488 nm.

2.9. HMGB1 release

Extracellular release of HMGB1 was measured using a high mobility

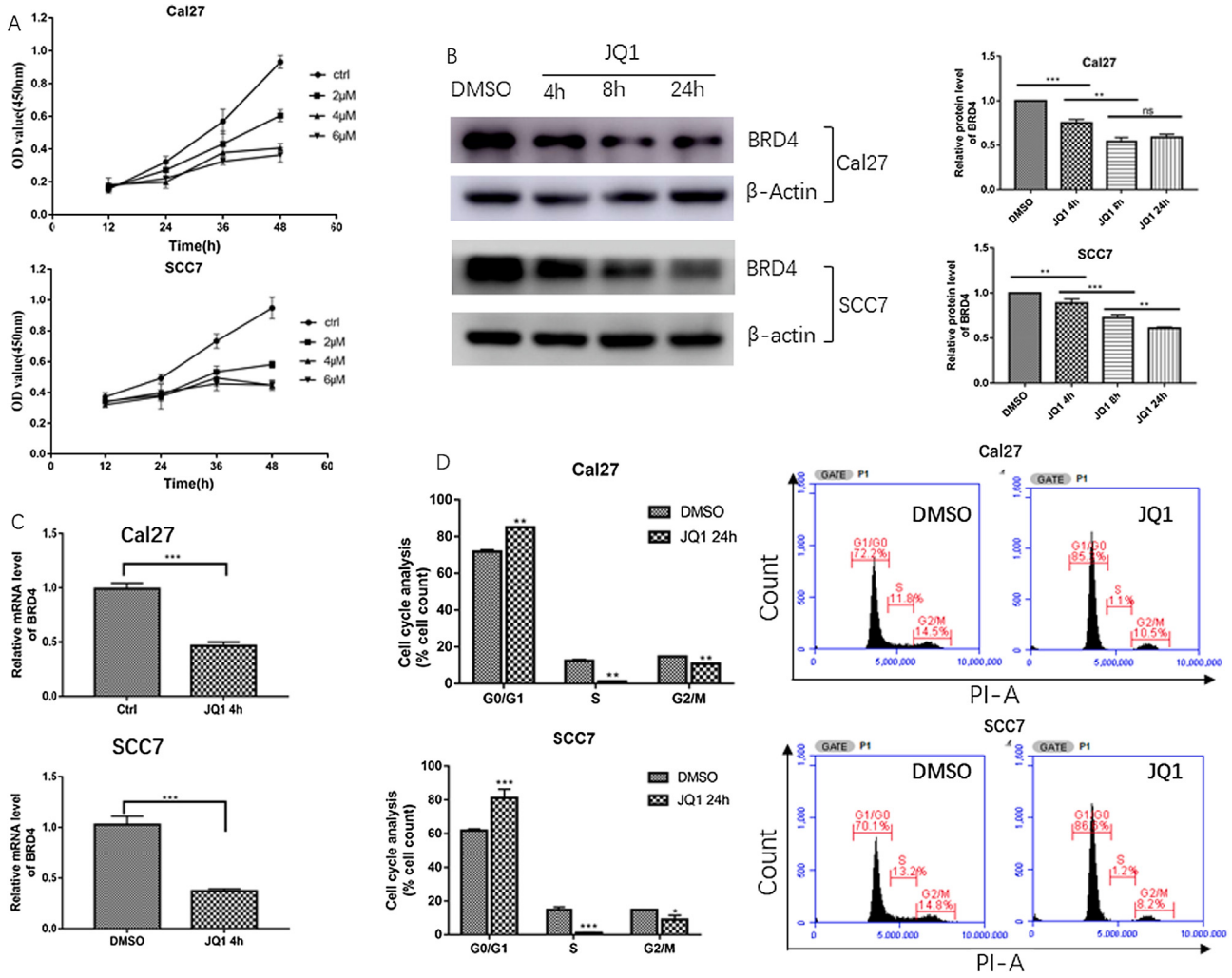

Fig. 1. Cell proliferation and cell cycling were significantly inhibited by JQ1. (A) Cell proliferation rate was measured using a CCK8 assay after treatment with various concentrations of JQ1. (B and C) Western blot analysis and qPCR data indicate that BRD4 was significantly inhibited by JQ1. Data represent means ± SEM of 3 replicate experiments. (***P < 0.005) (D) After incubation with JQ1 for 24 h, cells were collected to determine which stage of the cell cycle JQ1 targeted. Data represent means ± SEM of 3 replicate experiments (*P < 0.05, **P < 0.01, ***P < 0.001).

group protein 1 ELISA kit (USCN, Wuhan, China). Culture medium was collected after the cells had been treated with JQ1 for 24 h and 48 h. Samples were centrifuged for 20 min to eliminate debris and dead cells. Subsequent procedures were performed according to the manufacturer's instructions. OD levels were measured at 450 nm using a BMG SPECTROstar^{nano} scanning microplate reader. Results are expressed in ng/mL medium.

2.10. ATP assay

Cal27 or SCC7 cells were seeded in a 96-well plate at a density of 2×10^4/well. After incubation for 24 h, the medium was changed to serum-free DMEM and then JQ1 was added after specified time intervals (1 h, 2 h, 4 h and 24 h). Finally, ATP levels (extracellular and total) were quantified using a luciferase-based ATP assay kit (Promega, Madison, WI, USA) in accordance with the manufacturer's instructions. To measure total ATP production, cells were firstly lysed. Bioluminescence was measured using a Centro XS^3 LB960 microplate reader (Berthold Technologies, Bad Wildbad, Germany).

2.11. Immunofluorescence

Cells were seeded in confocal dishes. After incubation with JQ1 for 4 h, cells were washed twice with cold PBS then fixed in 0.5% PFA for 10 min. Cells were washed with 1% BSA/PBS and blocked using 5% goat serum (Boster, Wuhan, China) for 30 min. The goat serum was then discarded and the samples incubated with fluorescence-labelled anti-CALR primary antibody (1:100, diluted in 1% BSA) at 4 °C, overnight. The cells were washed in cold 1% BSA/PBS three times and incubated with a secondary antibody conjugated with Alexa Fluor® 488 (Abcam) for 30 min at room temperature in the dark. Subsequently, the cells were incubated with 10 μM Hoechst 33342 (BD Pharmingen) for 15 min to stain the nuclei. Finally, the cells were washed several times and immediately observed using a LSM780 confocal microscope (Carl Zeiss AR, Oberkochen, Germany).

2.12. Western blot analysis

Cells were lysed using RIPA buffer (Solarbio, Beijing, China) to extract proteins then broad spectrum protease (Boster) and phosphatase inhibitors (Boster) were added to prevent protein degradation. Membrane proteins were extracted using a specific Mem-PER™ Plus membrane protein extraction kit (Pierce, Bronze Way, Dallas, USA) in accordance with the manufacturer's instructions. Protein concentration was quantified using a BCA protein assay kit (Pierce). Proteins (30 μg) were electrophoresed through precast bis-Tris polyacrylamide gels (8%,

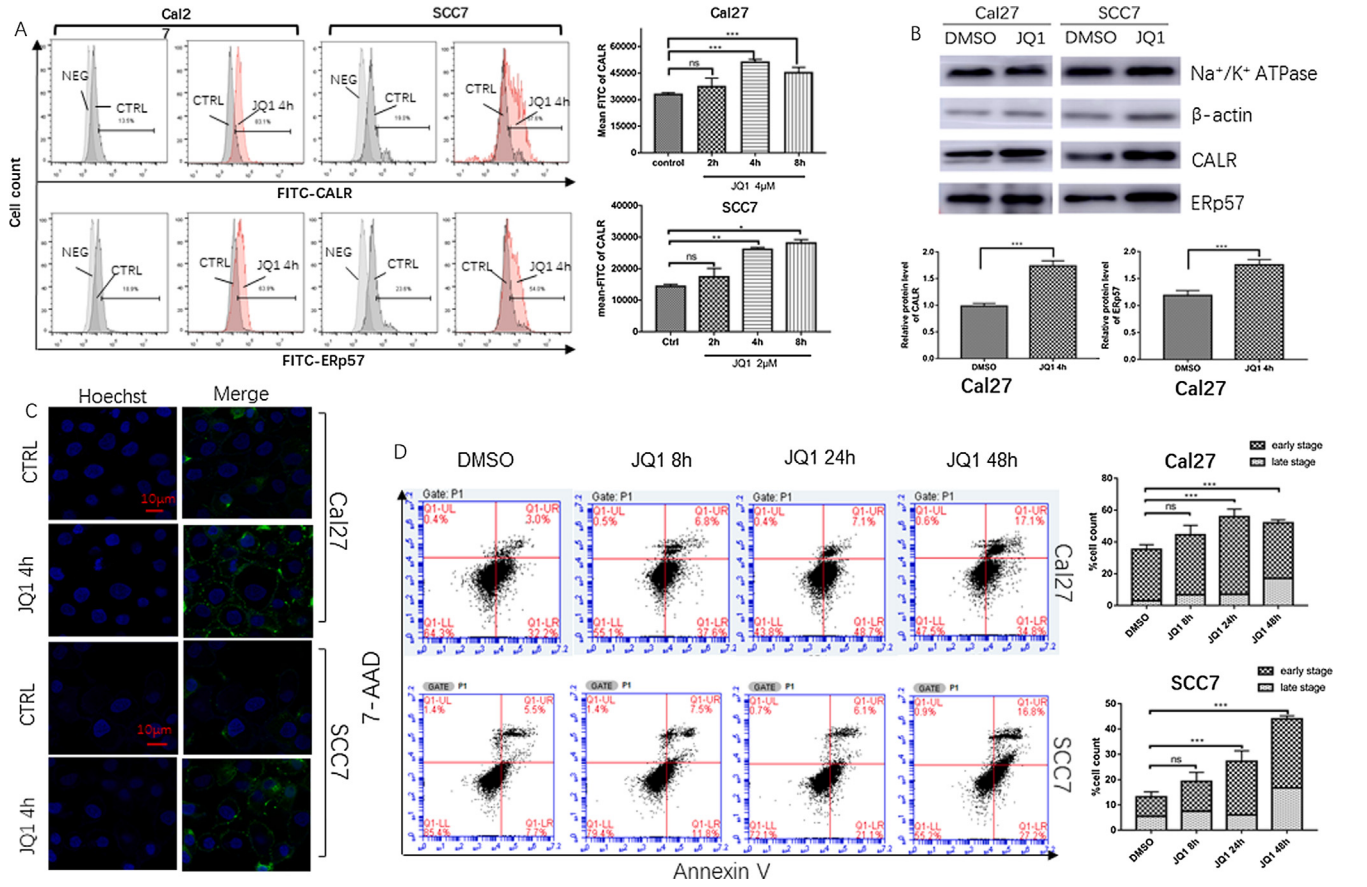

Fig. 2. JQ1 induced CALR/ERp57 translocation within 4 h. (A) Representative peaks of ecto-CALR/ERp57 and values of mean FITC fluorescence of CALR at different time points. Percentages of positive cells are shown. Light gray histograms represent negative controls while dark histograms represent DMSO controls. Mean FITC values of CALR at different time points are means ± SEM of 3 replicate experiments (*P < 0.05, **P < 0.01, ***P < 0.001). (B) Cell membrane proteins were extracted and analyzed by Western blotting; Na + /K + -ATPase was used as a loading control; β-actin was used to exclude intracellular proteins. Quantitative data of ecto-CALR/ERp57 expression are shown as means ± SEM of 3 independent experiments. (C) The immunofluorescence study indicated significant upregulation of CALR on cell membranes after treatment with JQ1. (D) Apoptosis assay by flow cytometry indicated that there was no significant phosphatidylserine exposure until 24 h and that apoptosis was mainly at an early stage; data represent means ± SEM of 3 replicate experiments (***P < 0.001).

10% or 12% for different molecular weight ranges) then transferred to PVDF membranes. Non-specific binding to the membranes was blocked by 5% non-fat milk which were then probed with the following panel of antibodies: anti-β-actin (Easybio, Beijing, China), anti-Na^+/K^+-ATPase α (CST, Danvers, MA, USA), anti-human BRD4 (CST), anti-mouse BRD4 (Abcam), anti-calreticulin (CST), anti-ERp57 (CST), anti-HMGB1 (CST), anti-PERK (CST), anti-P-PERK (Biolegend, San Diego, CA , USA), anti-mouse P-PERK (CST), anti-eIF2α (CST) and anti-P-eIF2α (CST). After incubation at 4 °C overnight, PVDF membranes were washed three times for a total of 30 min and incubated with secondary goat anti-rabbit (Boster, Wuhan, China) or goat anti–mouse (Boster) antibodies conjugated with HRP for 1 h. The membranes were then washed and imaged using an ImageQuant LAS4000 imager (GE Healthcare, USA) using a chemiluminescent HRP substrate (Millipore, WBKLS0500).

2.13. Dendritic cell culture

Immature DCs were generated from PBMCs using plastic adherence, as described previously [29–32] for subsequent maturation analysis. Briefly, human PBMCs were isolated from 50 mL whole blood from healthy donors by centrifugation through a Ficoll-Hypaque density gradient (TBD, Tianjin, China). Isolated cells were resuspended in RPMI-1640 supplemented with 1% human AB serum (Genenode, Beijing, China), seeded in a 6-well plate at a density of 1×10^6 cells/well and cultured in an incubator for 2 h. The cells were then washed several times to remove unattached cells. Finally, PBMCs were induced using 50 ng/mL GM-CSF and 20 ng/mL IL-4 (Peprotech, Rocky Hill, NJ, USA) for 7 days and analyzed by flow cytometry. The medium was partially replaced every other day, the correct quantity of supplementary cytokines also added. This experiment was approved by the Research Ethic Committee of Shandong University Dental School (GR201818). Informed consent was signed from each volunteer before the experiments.

2.14. Cell coculture

After induction for 6 days, immature DCs were added to Cal27 cells and cocultured for 36 h. Cal27 cells in the experimental group were pretreated with JQ1 for 4 h. The cells were then washed several times to completely remove JQ1. LPS (Sigma, USA) was added at a concentration of 1 μg/mL as the positive control group. DCs were treated with 0.25 μM JQ1 for 4 h, as a control, to ascertain whether JQ1 could directly promote maturation of DCs. The cells were collected and stained with CD86-APC and HLA-DR-FITC (BD Pharmingen, USA) then incubated at 4 °C for 30 min in the dark. Finally, the cells were washed three times, resuspended in 400 μL PBS and immediately assayed by flow cytometry. Culture media were collected from cell cultures to measure the human IL-6, human IL-12p70 and human IL-23 secreted by DCs using ELISA kits purchased from Dakewe Bio-engineering Co., Shenzhen Province, China.

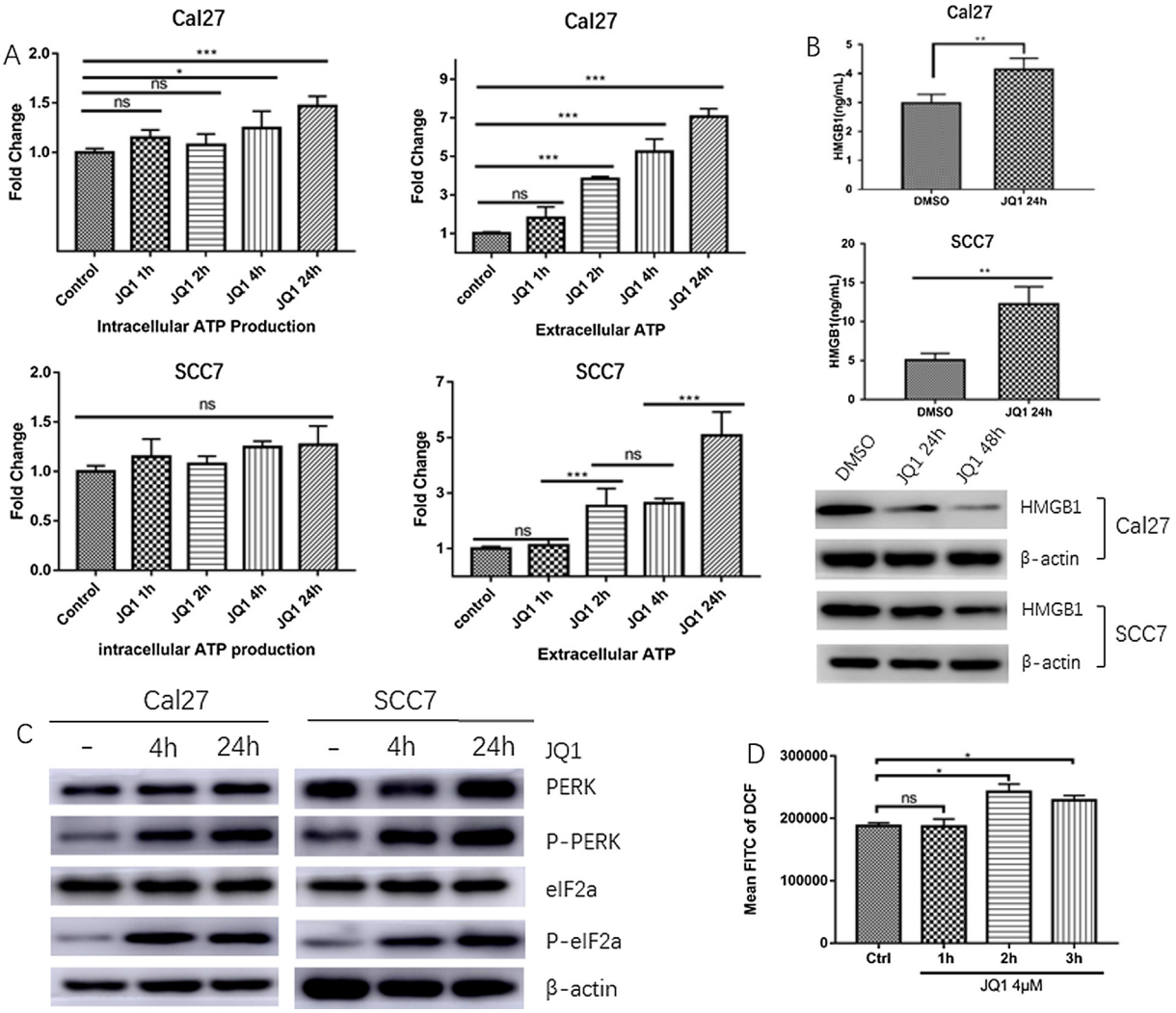

Fig. 3. JQ1 induced release of ATP and HMGB1 in addition to eIF2a phosphorylation. (A) Cell lysis buffer was used to measure total ATP production. All data were normalized against the luminescence of the DMSO control group (set to a value of 1). Data represent means ± SEM of 3 replicate experiments (**P < 0.01; ***P < 0.001). (B) HMGB1 release measured by ELISA and intracellular protein expression levels of HMGB1 by Western blot analysis. Data represent means ± SEM of 3 replicate experiments (**P < 0.01). (C) Levels of phosphorylated PERK and eIF2a increased significantly after incubation with JQ1 for 4 h. (D) DCF assay by cytometry indicates immediate increase in ROS levels in Cal27 cells. Data represent means ± SEM of 3 replicate experiments (*P < 0.05).

2.15. Antitumor vaccination assay

To determine if JQ1-treated SCC7 cells could protect the mice against rechallenge from the same tumor cells, C3H mice and Nu/Nu nude mice were inoculated with JQ1-treated SCC7 cells, as previously reported [11,12,33]. The SCC7 cells were pretreated with JQ1 (2 μM) for 24 h. Treated dying SCC7 cells (3×10^6 in 150 μL PBS) were inoculated subcutaneously into the lower right flank of 10 five-week-old female C3H mice and 10 five-week-old female Nu/Nu nude mice. An additional 10 C3H mice and 10 Nu/Nu nude mice were s.c. injected with 150 μL PBS as controls. A second inoculation was performed after 1 week to the same site. Finally, approximately 5×10^5 SCC7 cells were *s.c.* inoculated into the left side 7 days after the second immunization. Tumor-free mice were examined every 5 days. After 50 days, the mice were sacrificed and tumors on the left side dissected to observe size differences among the four groups described above. All experiments were approved by the Research Ethic Committee of Shandong University Dental School (GD201821).

2.16. Chemotherapeutic effect of JQ1 compared with established cancer models

SCC7 cells (5×10^5) were *s.c.* injected into the right flank of C3H or Nu/Nu nude mice which were randomly allocated into control or treatment groups, each group comprising 5 mice. When the volume of tumors had reached 80 mm^3 (calculated as $V = a \times b^2/2$, where a represented the maximum dimension and b was the minimum dimension), mice were administrated 50 mg/kg JQ1 or an equal volume of DMSO (150 μL), as appropriate, by caudal vein injection every other day over a 3-week period. Tumor size was monitored with a caliper every 2–3 days until day 30. All mice were then euthanized and tumors harvested, weighed and sectioned. All experiments were approved by the Research Ethic Committee of Shandong University Dental School (GD201821).

2.17. Immunohistochemistry

Tumors from C3H mice were fixed in formaldehyde, paraffin-embedded then sliced into 4 μm sections. Samples were processed using routine staining procedures, utilizing an HRP/DAB IHC detection kit (Abcam). After antigen retrieval in sodium citrate buffer (pH 6.0) for

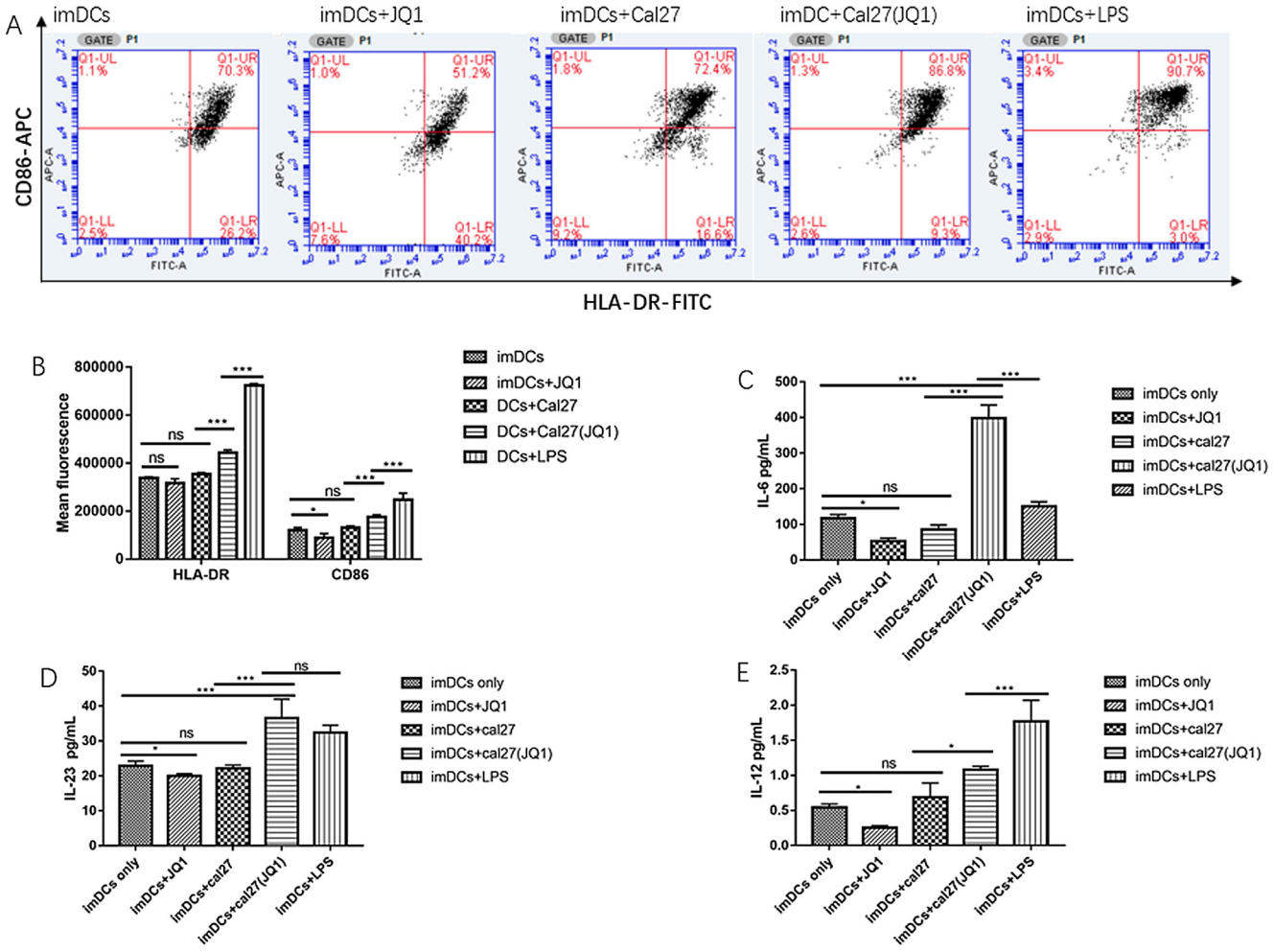

Fig. 4. Co-culture of Cal27 cells and im-DCs demonstrated that JQ1 altered the immunogenicity of Cal27 cells. (A and B) Flow cytometry results indicated significant upregulation of HLA-DR and CD86 on DCs after im-DCs were co-cultured with JQ1-pretreated Cal27 cells. Data represent means ± SEM of 3 independent experiments (**P < 0.01, ***P < 0.001). (C-E) ELISA of IL-6, IL-23 and IL-12 in the culture medium of im-DCs, im-DCs with untreated Cal27cells, im-DCs with JQ1-pretreated Cal27cells, JQ1-treated DCs and LPS-treated DCs. Data represent means ± SEM of 3 independent experiments (*P < 0.05, ***P < 0.001).

10 min at 100 °C, sections were stained with anti CD8 (Servicebio, Wuhan, China) and anti CD3 antibodies (Servicebio, Wuhan, China) at 4 °C overnight, incubated in biotinylated anti-rabbit secondary antibody and then in HRP-labeled-streptavidin using standard methods. Finally, CD3 and CD8 were visualized using DAB. Sections were briefly counterstained with hematoxylin for 1 min. Sections were observed using a light microscope (Olympus CX23, Japan). Numbers of CD3 or CD8 positive cells were counted.

2.18. Statistical analysis

Statistics were analyzed using GraphPad Prism 7. All data are represented using means ± SEM of triplicate experiments. The statistical significance between two groups was calculated using an unpaired Student's *t*-test. Multiple groups were compared using a one-way ANOVA followed by a Tukey's multiple comparison test. Specific software (Curve export 1.4) was used for to curve fit ELISA standards. Specific P values are denoted in this study as follows: *P < 0.05; **P < 0.01; ***P < 0.001. P < 0.05 was considered statistically significant.

3. Results

3.1. JQ1 induces cell cycle arrest

The BRD4 expression levels in Cal27 and SCC7 cells were quantified at various time intervals after treatment with JQ1. A CCK8 assay was performed in advance to determine appropriate working concentrations for JQ1. Concentrations of 4 μM and 2 μM were optimum for Cal27 and SCC7 cells, respectively (Fig. 1A). mRNA and protein expression levels of BRD4 were significantly suppressed by JQ1 after 4 h (Fig. 1B and C). To analyze the effect of JQ1 on the cell cycle, cells were treated with JQ1 for 24–48 h. Flow cytometry results displayed a dramatic decrease in the percentage of cells in the S phase and a corresponding decrease of those in the G2/M phase (Fig. 1D). A significant increase in the percentage of cells in the G0/G1 phase was also observed. These data indicate that JQ1 strongly blocked the cell cycle at the G1 phase.

3.2. JQ1 induces CALR/ERp57 translocation prior to apoptosis

Flow cytometry indicated that JQ1 induced exposure of CALR/ERp57 within 4 h or less (Fig. 2A). Additional analysis of cell membrane proteins by Western blot analysis and immunofluorescence demonstrated similar results (Fig. 2B and C). However, JQ1 at the same concentration did not induce significant apoptosis in Cal27 or SCC7 cells until 24 h and principally triggered the early stages of apoptosis

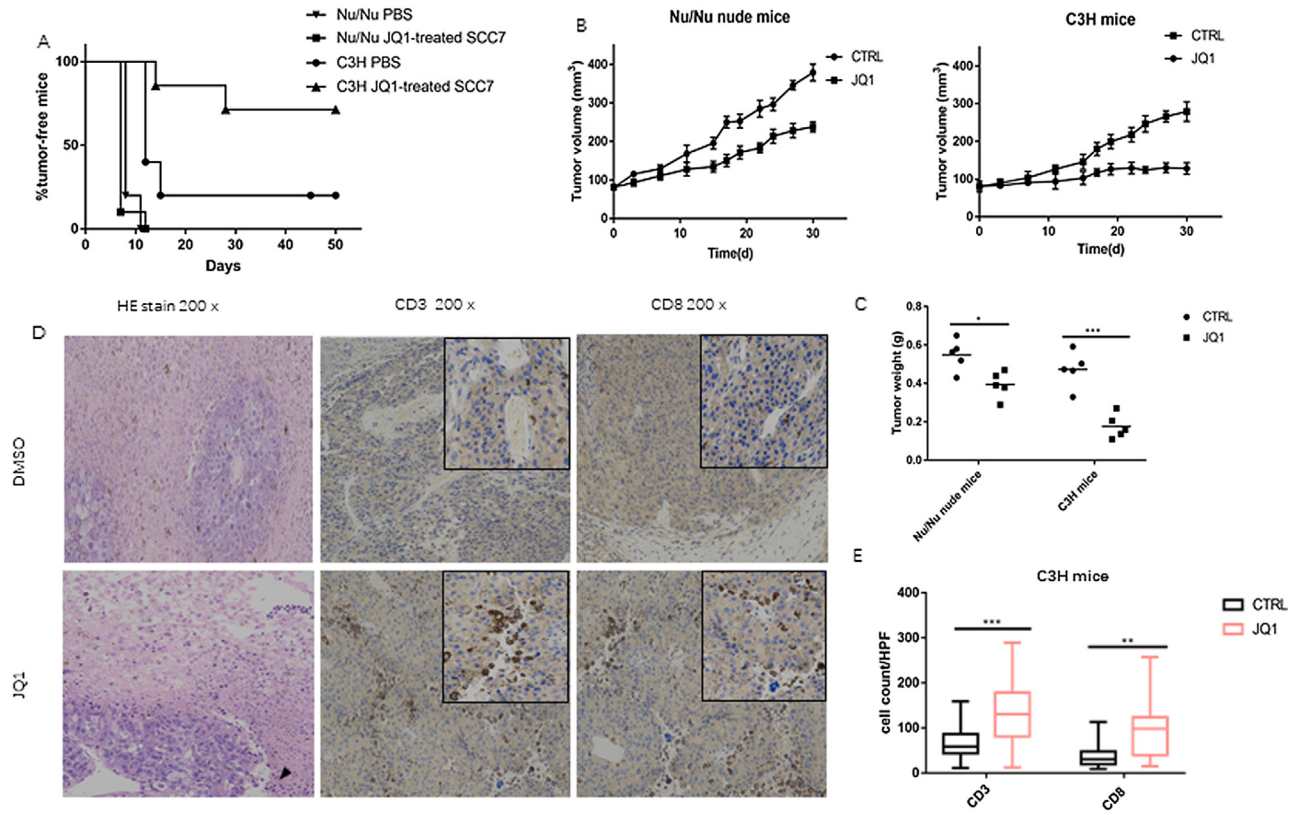

Fig. 5. JQ1-induced immunogenic cell death of tumor cells *in vivo*. (A) Anti-tumor inoculation experiments indicated that immunocompetent mice developed immunity to SCC7 cells after two inoculations of JQ1-treated dying SCC7 cells. Each group comprised 10 five-week-old female mice. (B) Tumor volumes measured every 2–3 days in nude mouse models or immunocompetent mouse models. Each group consisted of 5 five-week-old female mice. Data represent means ± SEM of tumors in 5 five-week-old female mice. (C) Tumor weight in control and JQ1 groups in nude and C3H mice (*P < 0.05, ***P < 0.001). (D) Anti-CD3 and anti-CD8 staining in immunohistochemistry indicated greater CD3 + /CD8 + T cell infiltration after treatment with JQ1. (E) Quantitative analysis of CD3 + and CD8 + T cells per high-power field (HPF). Data represent the median of 20 HPFs with 95% CI (**P < 0.01, ***P < 0.001).

(Fig. 2D). Significant cell shrinkage was observed by microscopy after 36 h, implying the induction of ecto-CALR/ERp57 was independent of exposure of phosphatidylserine.

3.3. JQ1 induces release of ATP and HMGB1

A luciferase-based ATP assay indicated that JQ1 induced ATP release in both cell lines within 2 h. Extracellular ATP accumulated to a quantity of approximately 7 and 5 folds greater than that of the DMSO control groups after 24 h in Cal27 and SCC7 cells, respectively. Interestingly, intracellular ATP production displayed no significant decline but a slight increase (Fig. 3A). The increase in ATP generation can be credited to a reprogramming of cellular metabolism [34], a common phenomenon in invasive neoplasia with high malignancy which helps tumor cells survive under critical conditions. A specific ELISA kit was used to measure HMGB1 within the culture medium. The results demonstrated significantly increased HMGB1 release after 24 h (Fig. 3B). However, the levels of intracellular HMGB1 protein measured by Western blot analysis declined significantly (Fig. 3B), indicating that JQ1 induced release but not expression of HMGB1.

3.4. JQ1 induces phosphorylation of PERK/eIF2a

As a hallmark of ICD, P-eIF2a is required for CALR translocation [5]. Here, we detected significant activation of PERK and subsequent phosphorylation of eIF2a within 4 h (Fig. 3C), further confirming that JQ1 was able to induce ICD in Cal27 and SCC7 cells. More significantly, JQ1 led to immediate ROS generation in Cal27 cells (Fig. 3D) within 2 h. ROS-induced ICD usually manifests more efficient ecto-CALR induction [35], but JQ1 did not increase levels of ROS in the SCC7 murine cell line.

3.5. JQ1-treated Cal27 cells promote maturation of im-DCs

To ascertain whether JQ1 was able to more directly improve the immunogenicity of tumor cells, we cocultured immature human dendric cells (im-DCs) with JQ1-pretreated Cal27 cells. im-DCs were derived from 5 healthy donors. After incubation for 36 h, mature DC cell surface markers (CD86 and HLA-DR) were measured by flow cytometry, the results demonstrating a significant increase in CD86 and HLA-DR expression on the surface of DCs (Fig. 4A and B). LPS was used as a positive control. The expression of CD86 and HLA-DR on DCs cultured with JQ1-pretreated Cal27 cells was significantly higher than on DCs cultured with untreated Cal27 cells. Since there were no significant differences in CD86 and HLA-DR expression on the surface of DCs in the groups comprising DCs only and those co-cultured with untreated Cal27 cells, it is reasonable to conclude that Cal27 cells themselves exhibited poor immunogenicity and were not able to activate DCs. To ascertain whether JQ1 could directly promote the maturation of im-DCs, JQ1 (0.25 μM) was added to im-DCs for 4 h. It was confirmed that CD86 expression reduced significantly and HLA-DR expression of im-DCs and im-DCs treated with JQ1 were not statistically different, confirming the conclusion that the change in Cal27 immunogenicity promoted DC maturation.

In addition, the presence of IL-6, IL-12 and IL-23 in the culture medium was quantified. Secretion levels of these cytokines increased significantly (Fig. 4C–E) after coculture of im-DCs with JQ1-pretreated Cal27 cells, compared with those of DCs cultured with untreated Cal27

or the DC only groups. However, JQ1 significantly reduced secretion of these cytokines when directly incubated with DCs at a concentration of 0.25 μM for 4 h, similar to observations of a previous study [30]. However, it should be noted that plastic adherence methods used here to enrich the precursor cell of DCs is not so efficient with an estimated purity about 72% [31].

3.6. In vivo studies

Inoculation experiments were conducted, as previously performed, to ascertain whether JQ1 treated-SCC7 cells could protect immunocompetent C3H/HeNcrl (C3H) mice from rechallenge by SCC7 cells. Two weeks after the second inoculation with dying SCC7 cells (incubated with JQ1 for 24 h), C3H mice developed immunity to SCC7 cells while the tumor cells were still able to grow in nude mice. After 50 days, 8 out of 10 immunocompetent C3H mice in the PBS control group had tumors, while only 3 out of 10 of the C3H mice in the inoculation group exhibited tumor formation (Fig. 5A).

To ascertain the chemotherapeutic effect of JQ1 *in vivo*, SCC mouse models were established via *s.c.* inoculation of SCC7 cells. As expected, tumor volume, as measured every 2–3 d was significantly reduced after intravenous injection of JQ1 both in nude and C3H mice (Fig. 5B). After 30 days, all mice were euthanized and tumors harvested. Those in the C3H mice were considerably smaller than those in the nude mice (volume: 127.91 cm^3 ± 14.99, weight: 0.176 g ± 0.028 and volume: 237.91 cm^3 ± 13.17, weight: 0.394 g ± 0.031, respectively; means ± SEM) after injection of JQ1 (Fig. 5C). Moreover, immunohistology (Fig. 5D and E) indicated that the number of tumor-infiltrating $CD3^+$ and $CD8^+$ T cells in the C3H mice injected with JQ1 (CD3: 134.50 ± 15.64; CD8: 95.50 ± 14.49, means ± SEM) was significantly higher than those in the DMSO controls (CD3: 64.45 ± 7.60; CD8: 38.90 ± 5.67, means ± SEM).

4. Discussion

Manipulating immunogenic response is an appealing method of treating tumors. In head and neck carcinomas such as TSCC, chemotherapy is often not as effective as expected due to drug resistance and impairment of the immune system. Surgery is generally regarded as the first choice to treat these cancers, leading to severe malfunction and facial deformity. Hence, restoration of the immunosurveillance system and alteration of the tumor microenvironment is a prospective way to improve multidisciplinary therapy of these cancers. In recent decades, a new pattern of cell death known as immunogenic apoptosis or ICD has been introduced. It is a procedure in which tumor cells undergo a change in immunogenicity with subsequent modification of the tumor microenvironment into one that is immune-active, allowing tumor cells to be killed by immunocytes and anti-tumor cytokines. In general, the majority of agent-induced apoptosis is nonimmunogenic whereas inducers of ICD are capable of eliciting the release of DAMPs, such as CALR, ATP and HMGB1, resulting in immunogenic apoptosis. Specifically, CALR, which is associated with the accumulation of unfolded proteins and functions as a signal of “eat me” [36,37], is capable of maturation of im-DCs and enhancing their phagocytic capability by binding to their toll-like receptors [38]. ATP is a “find me” signal which can recognize P2Y purinergic G protein-coupled receptor 2 (P2RY2) on phagocytes and DCs, enabling migration of these cells to the sites of inflammation [39–41]. HMGB1 is a postmortem DAMP of ICD, the reduced form of which can stimulate proinflammatory cytokines via TLR4 and advanced glycosylation end product-specific receptor (RAGE) on antigen-presenting cells (APCs) [42]. The central role of APCs, in particular DCs, is quite clear in immunogenic cell death, providing the ability to recognize CALR, engulf tumor cells, secret anti-tumor cytokines and activate T cells [43].

In this study, we demonstrated that the BRD4 inhibitor JQ1 was capable of inducing the release of CALR, ATP and HMGB1 in TSCC cells. In addition, two common markers of mature human DCs, CD86 and HLA-DR [44], were significantly upregulated after the coculture of im-DCs with JQ1-pretreated Cal27 cells, implying that JQ1 altered the immunogenicity of Cal27 cells via trigger of the release of DAMPs which promote the maturation of DCs, thus leading to an enhanced secretion activity. For example, secretion of the anti-tumor cytokines IL-6, IL-12 and IL-23 from DCs was significantly increased after co-culture with JQ1-pretreated Cal27 cells. These cytokines facilitate activation and migration of T cells, enhancing cytocidal activity of $CD8^+$ T cells (CTLs) [45]. Hence, *in vivo* studies were performed to ascertain whether JQ1 was able to induce an anti-tumor immune response in C3H mice. As expected, JQ1 effectively reduced tumor proliferation *in vivo*. Immunohistochemistry indicated that the C3H mice that received JQ1 treatment exhibited greater T cell infiltration in the tumor beds compared with the DMSO control. In addition, inoculation with JQ1 pretreated-SCC7 cells protected C3H mice from rechallenge by the same tumor cells, confirming that JQ1 could facilitate activation of the immune system via modulation of tumor immunogenicity. However, DCs acquired in the co-culture experiment were only monocyte-derived [46], neglecting other types of DCs with different phenotypes and biological behavior [43,47]. Hence, additional exploration of the individual roles of DC subtypes in ICD will assist in the production of more efficient DC vaccines and more accurate methods such as magnetic microbeads or cytometric selection should be used to improve purity of DCs instead of plastic adherence method used here.

An additional important finding is that phosphorylation of PERK/eIF2a, which is necessary for exposure of CALR [4,5,48,49], is significantly upregulated during JQ1-induced CALR traffic, demonstrating our supposition that JQ1 can induce ICD in TSCC through a molecular signal conduction mechanism. In addition, the immediate upregulation of ROS induced by JQ1 in Cal27 cells may have helped CALR transport because it is considered that ROS-induced ICD exhibits more efficient exposure of CALR [35]. By targeting the chromatin-binding protein BRD4, JQ1 triggers ICD through secondary ER stress instead of direct action at the ER (as occurs with photodynamic therapy). Therefore, JQ1-induced ICD can be classified as type I which usually involves convergence of ER stress and apoptosis [35]. In fact, an earlier study has confirmed that JQ1 is able to induce immunogenic cell death in malignant pleural mesothelioma [50], but no specific mechanism or influencing factors of JQ1-triggered CALR translocation or ATP release have been proposed. Therefore, a considerable degree of investigation is required to establish the mechanism of JQ1-induced ICD.

Acknowledgements

Special appreciation is given for the help of Dr. Gao, Professor of Immunology of Shandong University and Dr. Wang, Professor of Pathology of Shandong University Stomatology Hospital.

Funding

This work was supported by the National Natural Science Foundation of China (81802709); the Shandong Provincial Natural Science Foundation, China (ZR2018MH023 and ZR2018BH024); the Key Research and Development Plan of Shandong Province (2017GSF218064); the Shandong Provincial Postdoctoral Science Foundation (ZR2018BH024); the Program of Shandong University (2017JC010) and the Natural Science Foundation of Jinan (201704130 and 201805046).

Declaration of Competing Interest

The authors have no conflict to disclose.

References

[1] J. Fucikova, P. Kralikova, A. Fialova, T. Brtnicky, L. Rob, J. Bartunkova, R. Spisek, Human tumor cells killed by anthracyclines induce a tumor-specific immune response, Cancer Res. 71 (14) (2011) 4821–4833, https://doi.org/10.1158/0008-5472.can-11-0950.

[2] A. Tesniere, F. Schlemmer, V. Boige, O. Kepp, I. Martins, F. Ghiringhelli, L. Aymeric, M. Michaud, L. Apetoh, L. Barault, J. Mendiboure, J.P. Pignon, V. Jooste, P. van Endert, M. Ducreux, L. Zitvogel, F. Piard, G. Kroemer, Immunogenic death of colon cancer cells treated with oxaliplatin, Oncogene 29 (4) (2010) 482–491, https://doi.org/10.1038/onc.2009.356.

[3] Y. Zheng, G. Yin, V. Le, A. Zhang, S. Chen, X. Liang, J. Liu, Photodynamic-therapy activates immune response by disrupting immunity homeostasis of tumor cells, which generates vaccine for cancer therapy, Int. J. Biol. Sci. 12 (1) (2016) 120–132, https://doi.org/10.7150/ijbs.12852.

[4] L. Bezu, A. Sauvat, J. Humeau, L.C. Gomes-da-Silva, K. Iribarren, S. Forveille, P. Garcia, L. Zhao, P. Liu, L. Zitvogel, L. Senovilla, O. Kepp, G. Kroemer, eIF2alpha phosphorylation is pathognomonic for immunogenic cell death, Cell Death Differ. 25 (8) (2018) 1375–1393, https://doi.org/10.1038/s41418-017-0044-9.

[5] O. Kepp, M. Semeraro, J.M. Bravo-San Pedro, N. Bloy, A. Buque, X. Huang, H. Zhou, L. Senovilla, G. Kroemer, L. Galluzzi, eIF2alpha phosphorylation as a biomarker of immunogenic cell death, Semin. Cancer Biol. 33 (2015) 86–92, https://doi.org/10.1016/j.semcancer.2015.02.004.

[6] M. Obeid, A. Tesniere, T. Panaretakis, R. Tufi, N. Joza, P. van Endert, F. Ghiringhelli, L. Apetoh, N. Chaput, C. Flament, E. Ullrich, S. de Botton, L. Zitvogel, G. Kroemer, Ecto-calreticulin in immunogenic chemotherapy, Immunol. Rev. 220 (2007) 22–34, https://doi.org/10.1111/j.1600-065X.2007.00567.x.

[7] M. Obeid, A. Tesniere, F. Ghiringhelli, G.M. Fimia, L. Apetoh, J.-L. Perfettini, M. Castedo, G. Mignot, T. Panaretakis, N. Casares, D. Métivier, N. Larochette, P. van Endert, F. Ciccosanti, M. Piacentini, L. Zitvogel, G. Kroemer, Calreticulin exposure dictates the immunogenicity of cancer cell death, Nat. Med. 13 (2006) 54, https://doi.org/10.1038/nm1523 https://www.nature.com/articles/nm1523#supplementary-information.

[8] L. Senovilla, I. Vitale, I. Martins, M. Tailler, C. Pailleret, M. Michaud, L. Galluzzi, S. Adjemian, O. Kepp, M. Niso-Santano, S. Shen, G. Marino, A. Criollo, A. Boileve, B. Job, S. Ladoire, F. Ghiringhelli, A. Sistigu, T. Yamazaki, S. Rello-Varona, C. Locher, V. Poirier-Colame, M. Talbot, A. Valent, F. Berardinelli, A. Antoccia, F. Ciccosanti, G.M. Fimia, M. Piacentini, A. Fueyo, N.L. Messina, M. Li, C.J. Chan, V. Sigl, G. Pourcher, C. Ruckenstuhl, D. Carmona-Gutierrez, V. Lazar, J.M. Penninger, F. Madeo, C. Lopez-Otin, M.J. Smyth, L. Zitvogel, M. Castedo, G. Kroemer, An immunosurveillance mechanism controls cancer cell ploidy, Science 337 (6102) (2012) 1678–1684, https://doi.org/10.1126/science.1224922.

[9] H. Fang, B. Ang, X. Xu, X. Huang, Y. Wu, Y. Sun, W. Wang, N. Li, X. Cao, T. Wan, TLR4 is essential for dendritic cell activation and anti-tumor T-cell response enhancement by DAMPs released from chemically stressed cancer cells, Cell. Mol. Immunol. 11 (2) (2014) 150–159, https://doi.org/10.1038/cmi.2013.59.

[10] A.D. Garg, P. Agostinis, Cell death and immunity in cancer: from danger signals to mimicry of pathogen defense responses, Immunol. Rev. 280 (1) (2017) 126–148, https://doi.org/10.1111/imr.12574.

[11] O. Kepp, L. Senovilla, I. Vitale, E. Vacchelli, S. Adjemian, P. Agostinis, L. Apetoh, F. Aranda, V. Barnaba, N. Bloy, L. Bracci, K. Breckpot, D. Brough, A. Buque, M.G. Castro, M. Cirone, M.I. Colombo, I. Cremer, S. Demaria, L. Dini, A.G. Eliopoulos, A. Faggioni, S.C. Formenti, J. Fucikova, L. Gabriele, U.S. Gaipl, J. Galon, A. Garg, F. Ghiringhelli, N.A. Giese, Z.S. Guo, A. Hemminki, M. Herrmann, J.W. Hodge, S. Holdenrieder, J. Honeychurch, H.M. Hu, X. Huang, T.M. Illidge, K. Kono, M. Korbelik, D.V. Krysko, S. Loi, P.R. Lowenstein, E. Lugli, Y. Ma, F. Madeo, A.A. Manfredi, I. Martins, D. Mavilio, L. Menger, N. Merendino, M. Michaud, G. Mignot, K.L. Mossman, G. Multhoff, R. Oehler, F. Palombo, T. Panaretakis, J. Pol, E. Proietti, J.E. Ricci, C. Riganti, P. Rovere-Querini, A. Rubartelli, A. Sistigu, M.J. Smyth, J. Sonnemann, R. Spisek, J. Stagg, A.Q. Sukkurwala, E. Tartour, A. Thorburn, S.H. Thorne, P. Vandenabeele, F. Velotti, S.T. Workenhe, H. Yang, W.X. Zong, L. Zitvogel, G. Kroemer, L. Galluzzi, Consensus guidelines for the detection of immunogenic cell death, Oncoimmunology 3 (9) (2014) e955691, , https://doi.org/10.4161/21624011.2014.955691.

[12] T. Panaretakis, O. Kepp, U. Brockmeier, A. Tesniere, A.C. Bjorklund, D.C. Chapman, M. Durchschlag, N. Joza, G. Pierron, P. van Endert, J. Yuan, L. Zitvogel, F. Madeo, D.B. Williams, G. Kroemer, Mechanisms of pre-apoptotic calreticulin exposure in immunogenic cell death, Embo J. 28 (5) (2009) 578–590, https://doi.org/10.1038/emboj.2009.1.

[13] T. Panaretakis, N. Joza, N. Modjtahedi, A. Tesniere, I. Vitale, M. Durchschlag, G.M. Fimia, O. Kepp, M. Piacentini, K.U. Froehlich, P. van Endert, L. Zitvogel, F. Madeo, G. Kroemer, The co-translocation of ERp57 and calreticulin determines the immunogenicity of cell death, Cell Death Diff. 15 (2008) 1499, https://doi.org/10.1038/cdd.2008.67 https://www.nature.com/articles/cdd200867#supplementary-information.

[14] J.E. Delmore, G.C. Issa, M.E. Lemieux, P.B. Rahl, J. Shi, H.M. Jacobs, E. Kastritis, T. Gilpatrick, R.M. Paranal, J. Qi, M. Chesi, A.C. Schinzel, M.R. McKeown, T.P. Heffernan, C.R. Vakoc, P.L. Bergsagel, I.M. Ghobrial, P.G. Richardson, R.A. Young, W.C. Hahn, K.C. Anderson, A.L. Kung, J.E. Bradner, C.S. Mitsiades, BET bromodomain inhibition as a therapeutic strategy to target c-Myc, Cell 146 (6) (2011) 904–917, https://doi.org/10.1016/j.cell.2011.08.017.

[15] J. Wang, Z. Liu, Z. Wang, S. Wang, Z. Chen, Z. Li, M. Zhang, J. Zou, B. Dong, J. Gao, L. Shen, Targeting c-Myc: JQ1 as a promising option for c-Myc-amplified esophageal squamous cell carcinoma, Cancer Lett. 419 (2018) 64–74, https://doi.org/10.1016/j.canlet.2018.01.051.

[16] X. Zhu, K. Enomoto, L. Zhao, Y.J. Zhu, M.C. Willingham, P. Meltzer, J. Qi, S.Y. Cheng, Bromodomain and extraterminal protein inhibitor JQ1 suppresses thyroid tumor growth in a mouse model, Clin. Cancer Res. 23 (2) (2017) 430–440, https://doi.org/10.1158/1078-0432.ccr-16-0914.

[17] S. Jostes, D. Nettersheim, M. Fellermeyer, S. Schneider, F. Hafezi, F. Honecker, V. Schumacher, M. Geyer, G. Kristiansen, H. Schorle, The bromodomain inhibitor JQ1 triggers growth arrest and apoptosis in testicular germ cell tumours in vitro and in vivo, J. Cell Mol. Med. 21 (7) (2017) 1300–1314, https://doi.org/10.1111/jcmm.13059.

[18] P.L. Garcia, A.L. Miller, K.M. Kreitzburg, L.N. Council, T.L. Gamblin, J.D. Christein, M.J. Heslin, J.P. Arnoletti, J.H. Richardson, D. Chen, C.A. Hanna, S.L. Cramer, E.S. Yang, J. Qi, J.E. Bradner, K.J. Yoon, The BET bromodomain inhibitor JQ1 suppresses growth of pancreatic ductal adenocarcinoma in patient-derived xenograft models, Oncogene 35 (7) (2016) 833–845, https://doi.org/10.1038/onc.2015.126.

[19] D.O. Adeegbe, Y. Liu, P.H. Lizotte, Y. Kamihara, A.R. Aref, C. Almonte, R. Dries, Y. Li, S. Liu, X. Wang, T. Warner-Hatten, J. Castrillon, G.C. Yuan, N. Poudel-Neupane, H. Zhang, J.L. Guerriero, S. Han, M.M. Awad, D.A. Barbie, J. Ritz, S.S. Jones, P.S. Hammerman, J. Bradner, S.N. Quayle, K.K. Wong, Synergistic immunostimulatory effects and therapeutic benefit of combined histone deacetylase and bromodomain inhibition in non-small cell lung cancer, Cancer Discov. 7 (8) (2017) 852–867, https://doi.org/10.1158/2159-8290.cd-16-1020.

[20] J. Shahbazi, P.Y. Liu, B. Atmadibrata, J.E. Bradner, G.M. Marshall, R.B. Lock, T. Liu, The Bromodomain inhibitor JQ1 and the Histone Deacetylase Inhibitor Panobinostat synergistically reduce N-Myc expression and induce anticancer effects, Clin. Cancer Res. 22 (10) (2016) 2534–2544, https://doi.org/10.1158/1078-0432.ccr-15-1666.

[21] S. Liao, O. Maertens, K. Cichowski, S.J. Elledge, Genetic modifiers of the BRD4-NUT dependency of NUT midline carcinoma uncovers a synergism between BETis and CDK4/6is, Genes Dev. 32 (17–18) (2018) 1188–1200, https://doi.org/10.1101/gad.315648.118.

[22] S. Warnakulasuriya, Global epidemiology of oral and oropharyngeal cancer, Oral. Oncol. 45 (4–5) (2009) 309–316, https://doi.org/10.1016/j.oraloncology.2008.06.002.

[23] D. Pulte, H. Brenner, Changes in survival in head and neck cancers in the late 20th and early 21st century: a period analysis, Oncologist 15 (9) (2010) 994–1001, https://doi.org/10.1634/theoncologist.2009-0289.

[24] P. Zhang, L. Zhang, H. Liu, L. Zhao, Y. Li, J.X. Shen, Q. Liu, M.Z. Liu, M. Xi, Clinicopathologic characteristics and prognosis of tongue squamous cell carcinoma in patients with and without a history of radiation for Nasopharyngeal Carcinoma: a matched case-control study, Cancer Res. Treat 49 (3) (2017) 695–705, https://doi.org/10.4143/crt.2016.317.

[25] L. Wang, X. Wu, P. Huang, Z. Lv, Y. Qi, X. Wei, P. Yang, F. Zhang, JQ1, a small molecule inhibitor of BRD4, suppresses cell growth and invasion in oral squamous cell carcinoma, Oncol. Rep. 36 (4) (2016) 1989–1996, https://doi.org/10.3892/or.2016.5037.

[26] C.-Y. Wang, P. Filippakopoulos, Beating the odds: BETs in disease, Trends Biochem. Sci. 40 (8) (2015) 468–479, https://doi.org/10.1016/j.tibs.2015.06.002.

[27] E. Delmore Jake, C. Issa Ghayas, E. Lemieux Madeleine, B. Rahl Peter, J. Shi, M. Jacobs Hannah, E. Kastritis, T. Gilpatrick, M. Paranal Ronald, J. Qi, M. Chesi, C. Schinzel Anna, R. McKeown Michael, P. Heffernan Timothy, R. Vakoc Christopher, P.L. Bergsagel, M. Ghobrial Irene, G. Richardson Paul, A. Young Richard, C. Hahn William, C. Anderson Kenneth, L. Kung Andrew, E. Bradner James, S. Mitsiades Constantine, BET Bromodomain inhibition as a therapeutic strategy to target c-Myc, Cell 146 (6) (2011) 904–917, https://doi.org/10.1016/j.cell.2011.08.017.

[28] L.S. Toni, A.M. Garcia, D.A. Jeffrey, X. Jiang, B.L. Stauffer, S.D. Miyamoto, C.C. Sucharov, Optimization of phenol-chloroform RNA extraction, MethodsX 5 (2018) 599–608, https://doi.org/10.1016/j.mex.2018.05.011.

[29] P.A. Videira, M. Silva, K.C. Martin, R. Sackstein, Ligation of the CD44 Glycoform HCELL on culture-expanded human monocyte-derived dendritic cells programs transendothelial migration, J. Immunol. 201 (3) (2018) 1030–1043, https://doi.org/10.4049/jimmunol.1800188.

[30] P.A. Toniolo, S. Liu, J.E. Yeh, P.M. Moraes-Vieira, S.R. Walker, V. Vafaizadeh, J.A. Barbuto, D.A. Frank, Inhibiting STAT5 by the BET bromodomain inhibitor JQ1 disrupts human dendritic cell maturation, J. Immunol. 194 (7) (2015) 3180–3190, https://doi.org/10.4049/jimmunol.1401635.

[31] T. Felzmann, V. Witt, D. Wimmer, G. Ressmann, D. Wagner, P. Paul, K. Huttner, G. Fritsch, Monocyte enrichment from leukapharesis products for the generation of DCs by plastic adherence, or by positive or negative selection, Cytotherapy 5 (5) (2003) 391–398, https://doi.org/10.1080/14653240310003053.

[32] F. Bracho, C. van de Ven, E. Areman, R.M. Hughes, V. Davenport, M.B. Bradley, J.W. Cai, M.S. Cairo, A comparison of ex vivo expanded DCs derived from cord blood and mobilized adult peripheral blood plastic-adherent mononuclear cells: decreased alloreactivity of cord blood DCs, Cytotherapy 5 (5) (2003) 349–361.

[33] J. Lu, X. Liu, Y.-P. Liao, F. Salazar, B. Sun, W. Jiang, C.H. Chang, J. Jiang, X. Wang, A.M. Wu, H. Meng, A.E. Nel, Nano-enabled pancreas cancer immunotherapy using immunogenic cell death and reversing immunosuppression, Nat. Commun. 8 (1) (2017) 1811, https://doi.org/10.1038/s41467-017-01651-9.

[34] S. Herzig, R.J. Shaw, AMPK: guardian of metabolism and mitochondrial homeostasis, Nat. Rev. Mol. Cell Biol. 19 (2) (2018) 121–135, https://doi.org/10.1038/nrm.2017.95.

[35] D.V. Krysko, A.D. Garg, A. Kaczmarek, O. Krysko, P. Agostinis, P. Vandenabeele, Immunogenic cell death and DAMPs in cancer therapy, Nat. Rev. Cancer 12 (12) (2012) 860–875, https://doi.org/10.1038/nrc3380.

[36] S. Johnson, M. Michalak, M. Opas, P. Eggleton, The ins and outs of calreticulin:

from the ER lumen to the extracellular space, Trends Cell Biol. 11 (3) (2001) 122–129.
[37] M. Obeid, A. Tesniere, F. Ghiringhelli, G.M. Fimia, L. Apetoh, J.L. Perfettini, M. Castedo, G. Mignot, T. Panaretakis, N. Casares, D. Metivier, N. Larochette, P. van Endert, F. Ciccosanti, M. Piacentini, L. Zitvogel, G. Kroemer, Calreticulin exposure dictates the immunogenicity of cancer cell death, Nat. Med. 13 (1) (2007) 54–61, https://doi.org/10.1038/nm1523.
[38] L. Apetoh, F. Ghiringhelli, A. Tesniere, M. Obeid, C. Ortiz, A. Criollo, G. Mignot, M.C. Maiuri, E. Ullrich, P. Saulnier, H. Yang, S. Amigorena, B. Ryffel, F.J. Barrat, P. Saftig, F. Levi, R. Lidereau, C. Nogues, J.-P. Mira, A. Chompret, V. Joulin, F. Clavel-Chapelon, J. Bourhis, F. André, S. Delaloge, T. Tursz, G. Kroemer, L. Zitvogel, Toll-like receptor 4–dependent contribution of the immune system to anticancer chemotherapy and radiotherapy, Nat. Med. 13 (2007) 1050, https://doi.org/10.1038/nm1622 https://www.nature.com/articles/nm1622#supplementary-information.
[39] I. Martins, Y. Wang, M. Michaud, Y. Ma, A.Q. Sukkurwala, S. Shen, O. Kepp, D. Metivier, L. Galluzzi, J.L. Perfettini, L. Zitvogel, G. Kroemer, Molecular mechanisms of ATP secretion during immunogenic cell death, Cell Death Differ. 21 (1) (2014) 79–91, https://doi.org/10.1038/cdd.2013.75.
[40] Y. Wang, I. Martins, Y. Ma, O. Kepp, L. Galluzzi, G. Kroemer, Autophagy-dependent ATP release from dying cells via lysosomal exocytosis, Autophagy 9 (10) (2013) 1624–1625, https://doi.org/10.4161/auto.25873.
[41] A.D. Garg, D.V. Krysko, T. Verfaillie, A. Kaczmarek, G.B. Ferreira, T. Marysael, N. Rubio, M. Firczuk, C. Mathieu, A.J. Roebroek, W. Annaert, J. Golab, P. de Witte, P. Vandenabeele, P. Agostinis, A novel pathway combining calreticulin exposure and ATP secretion in immunogenic cancer cell death, Embo J. 31 (5) (2012) 1062–1079, https://doi.org/10.1038/emboj.2011.497.
[42] H. Inoue, K. Tani, Multimodal immunogenic cancer cell death as a consequence of anticancer cytotoxic treatments, Cell Death Differ. 21 (1) (2014) 39–49, https://doi.org/10.1038/cdd.2013.84.
[43] A. Gardner, B. Ruffell, Dendritic cells and cancer immunity, Trends Immunol. 37 (12) (2016) 855–865, https://doi.org/10.1016/j.it.2016.09.006.
[44] V. Chabot, L. Martin, D. Meley, L. Sensebé, C. Baron, Y. Lebranchu, F. Dehaut, F. Velge-Roussel, Unexpected impairment of TNF-α-induced maturation of human dendritic cells in vitro by IL-4, J. Transl. Med. 14 (2016) 93, https://doi.org/10.1186/s12967-016-0848-2.
[45] L. Galluzzi, A. Buque, O. Kepp, L. Zitvogel, G. Kroemer, Immunogenic cell death in cancer and infectious disease, Nat. Rev. Immunol. 17 (2) (2017) 97–111, https://doi.org/10.1038/nri.2016.107.
[46] S. Di Blasio, I.M.N. Wortel, D.A.G. van Bladel, L.E. de Vries, T. Duiveman-de Boer, K. Worah, N. de Haas, S.I. Buschow, I.J.M. de Vries, C.G. Figdor, S.V. Hato, Human CD1c(+) DCs are critical cellular mediators of immune responses induced by immunogenic cell death, e1192739 e1192739, Oncoimmunology 5 (8) (2016), https://doi.org/10.1080/2162402X.2016.1192739.
[47] A. Götz, M.S. Tang, M.C. Ty, C. Arama, A. Ongoiba, D. Doumtabe, B. Traore, P.D. Crompton, Loke Pn, A. Rodriguez, Atypical activation of dendritic cells by Plasmodium falciparum, E10568 E10577, PNAS 114 (49) (2017), https://doi.org/10.1073/pnas.1708383114.
[48] L. Bezu, A. Sauvat, J. Humeau, M. Leduc, O. Kepp, G. Kroemer, eIF2alpha phosphorylation: a hallmark of immunogenic cell death, Oncoimmunology 7 (6) (2018) e1431089, , https://doi.org/10.1080/2162402x.2018.1431089.
[49] A.R. van Vliet, S. Martin, A.D. Garg, P. Agostinis, The PERKs of damage-associated molecular patterns mediating cancer immunogenicity: From sensor to the plasma membrane and beyond, Semin. Cancer Biol. 33 (2015) 74–85, https://doi.org/10.1016/j.semcancer.2015.03.010.
[50] C. Riganti, M.F. Lingua, I.C. Salaroglio, C. Falcomatà, L. Righi, D. Morena, F. Picca, D. Oddo, J. Kopecka, M. Pradotto, R. Libener, S. Orecchia, P. Bironzo, V. Comunanza, F. Bussolino, S. Novello, G.V. Scagliotti, F. Di Nicolantonio, R. Taulli, Bromodomain inhibition exerts its therapeutic potential in malignant pleural mesothelioma by promoting immunogenic cell death and changing the tumor immune-environment, e1398874 e1398874, Oncoimmunology 7 (3) (2017), https://doi.org/10.1080/2162402X.2017.1398874.